

# Chemical species generated by high-vacuum ion gauges cause strong doping of graphene

Christophe Caillier,<sup>1,2</sup> Dong-Keun Ki,<sup>1,2</sup> Yuliya Lisunova,<sup>1</sup> Iaroslav Gaponenko,<sup>1</sup> Patrycja Paruch,<sup>1, a)</sup> and Alberto F. Morpurgo<sup>1,2, b)</sup>

<sup>1)</sup> MaNEP-DPMC, Université de Genève, 24 quai Ernest-Ansermet, CH-1211 Geneva, Switzerland

<sup>2)</sup> GAP, Université de Genève, 24 quai Ernest Ansermet, CH-1211 Geneva, Switzerland

(Dated: 22 February 2013)

To minimize drifts caused by uncontrolled material absorption, graphene is often investigated under vacuum. Here we report an entirely unexpected phenomenon occurring in vacuum systems, namely strong n-doping of graphene due to chemical species generated by common ion high-vacuum gauges. The effect – reversible upon exposing graphene to air – is strong, as doping rates can largely exceed  $10^{12}$  cm<sup>-2</sup>/hour, depending on pressure and relative position of the gauge and graphene. It is important to be aware of the phenomenon, as its basic manifestation can be mistakenly interpreted as due to vacuum-induced desorption of p-dopants.

There is a broad consensus that the unique structural and electronic properties of graphene<sup>1,2</sup> have great potential for the development of opto-electronic applications.<sup>3–5</sup> Technological progress, however, will require significant improvements to control the material, its uniformity over large areas, and its stability over time.<sup>4,5</sup> The latter is particularly important because the true two-dimensionality of graphene strongly amplifies interactions with the environment, be it the supporting substrate, or unintentionally present adsorbates. While it seems clear that – to ensure the needed stability – an appropriate encapsulation strategy will have to be developed for future applications, most investigations of graphene are currently performed under high-vacuum conditions. In this case, desorption of adsorbates is the only process that is expected to cause time dependence of the measured properties of graphene, and time stability does not appear to be an issue.

In this paper we report the finding of an unexpected phenomenon that occurs under vacuum conditions, and that causes an extremely pronounced time instability in the electronic properties of graphene. Specifically, we have found that even in high-vacuum systems, emission of active chemical species produced by the filament of common ion pressure gauges can cause very large shifts in the gate voltage  $V_G$  at which the graphene charge neutrality point occurs. We have observed the effect to be present – and to manifest itself very similarly – on graphene obtained by both chemical vapor deposition<sup>6–12</sup> (CVD) and by exfoliation,<sup>13</sup> with changes in density of charge carriers much larger than  $10^{12}$  cm<sup>-2</sup>/hour. This gauge-induced doping can overcome the original p-doping of the material as measured in air (even when the initial doping level is very large), eventually making the material substantially n-doped. It can be completely reversed upon (re)exposure of graphene to air, without seemingly

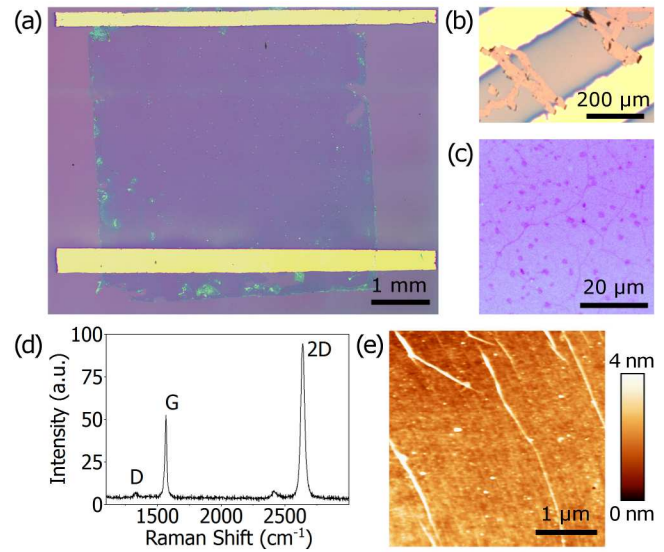


FIG. 1. (a) Large area CVD graphene sample contacted by Au/Ti electrodes evaporated through a shadow mask, with few PMMA residues from the transfer process visible as bright features near the edges. (b) Smaller device fabricated by cutting graphene with a needle, using a micro-manipulator in a probe-station. (c) High-magnification optical microscope image of a CVD graphene sample, showing wrinkles (dark lines) and small multilayer islands (dark spots). (d) Raman spectrum demonstrating the monolayer character of our CVD-grown samples. (e) Atomic force microscope of a sample transferred onto a Si/SiO<sub>2</sub> substrate, with a roughness of  $\sim 6$  Å. Small wrinkles a few nm high (white lines) and nanoparticle residues from the transfer process (white spots) are also visible.

causing any permanent damage to graphene. The phenomenon appears in all high vacuum systems where pressure is monitored via an ion gauge, as long as the chemical species generated by the ion gauge can reach the graphene sample before being pumped away (i.e., depending on the position of the ion gauge relative to the pumping system). Since such systems are widely used by

<sup>a)</sup> Electronic mail: Patrycja.Paruch@unige.ch

<sup>b)</sup> Electronic mail: Alberto.Morpurgo@unige.ch

many research groups working on the characterization of graphene, it is important to be aware of the existence of the phenomenon, to avoid misinterpreting results of experiments performed under vacuum conditions.

Most of the graphene samples investigated here were grown by low-pressure CVD<sup>6-9</sup> on a 25  $\mu\text{m}$  thick 99.999 % copper foil, following a two-step process derived from Ref. 7. The Cu foils are first annealed at 1000  $^{\circ}\text{C}$  under a 5 sccm  $\text{H}_2$  flow at 50 mTorr for 20 minutes. Then graphene is grown in 5 sccm  $\text{H}_2$  and 7 sccm  $\text{CH}_4$  at 1035  $^{\circ}\text{C}$ , with an initial 4 minute growth step at 120 mTorr, and a second step increasing the growth pressure to 1 Torr over 15 seconds. Finally, the pressure is decreased back to 120 mTorr, and the samples cooled under process gas flow for 30 minutes. These parameters have been optimized to produce homogeneous graphene monolayers, with only few multilayer islands or contaminating nano-particles.<sup>14</sup>

Using a PMMA-mediated technique derived from Liang *et al.*,<sup>15</sup> the graphene layers were transferred onto doped silicon substrates covered by 300 nm oxide. Under high magnification optical microscopy (Fig. 1(c)), the samples appear uniform, with wrinkles and small multilayer islands distinguishable, respectively, as dark lines and spots distributed all over the sample surface. Characterization of the sample topography by atomic force microscopy (Fig. 1(e)) shows low  $\sim 1$  nm surface roughness, with small wrinkles and nanoparticles from the transfer process. The monolayer character of the samples is confirmed through Raman spectroscopy measurements, shown in Fig. 1(d). A high intensity ratio between the 2D ( $2700\text{ cm}^{-1}$ ) and G ( $1580\text{ cm}^{-1}$ ) bands is found, as well as a single Lorentzian profile of the 2D peak, with a width at half maximum of  $34\text{ cm}^{-1}$ .<sup>16,17</sup> The small intensity of the D band ( $1350\text{ cm}^{-1}$ ) demonstrates that the CVD graphene is not disordered at small length scales.<sup>18</sup>

Two-terminal graphene devices were fabricated by the deposition of source and drain electrodes (10 nm Ti / 50 nm Au) through a shadow mask, allowing either the full samples with dimensions of about  $5\times 5\text{ mm}^2$ , or smaller  $200\times 200\text{ }\mu\text{m}^2$  areas, to be measured rapidly, without the need of any lithographic processing (Figs. 1(a) and 1(b); the doped Si substrate was used as gate contact). The samples were characterized in a *Lakeshore CPX* probe station under vacuum, with a cold cathode ion gauge mounted directly on the chamber. The resistance was obtained by current-biasing (100 nA at  $\sim 20\text{ Hz}$ ) the graphene devices, and measuring the source-drain voltage with an *SR830* lock-in amplifier. Over the large areas of our devices, the as-grown material reproducibly shows a field effect mobility  $\mu$  of approximately  $1000\text{ cm}^2\text{V}^{-1}\text{s}^{-1}$  at room temperature, increasing (also reproducibly) to approximately  $1400\text{ cm}^2\text{V}^{-1}\text{s}^{-1}$  after current annealing in vacuum. For comparison, we also investigated an exfoliated graphene sample with a dimension of approximately  $10\times 10\text{ }\mu\text{m}^2$  (with  $\mu \sim 1800\text{ cm}^2\text{V}^{-1}\text{s}^{-1}$ , which was selected to have a mobility value close to that of CVD-grown graphene).

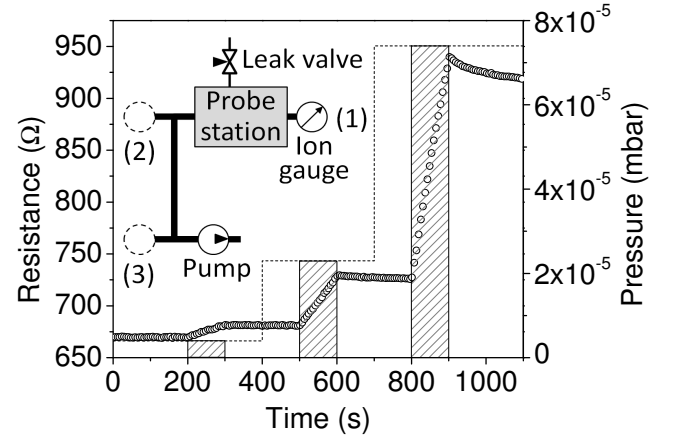


FIG. 2. Evolution of the resistance of a CVD device (open circles) upon turning on and off the ion gauge for different values of the pressure (dashed line) inside the chamber. The resistance increases when the ion gauge is on (shaded regions, the height of which corresponds to the pressure during the measurement), with a rate found to be higher at higher pressure. When the gauge is switched off, the resistance remains approximately constant. Inset: scheme of the vacuum chamber showing the position of the gauge (1) for this measurement. Dashed circles (2) and (3) indicate alternative positions of the gauge, displaced further away from the sample, on the pumping line (see discussion in main text).

In order to distinguish between the effects of the ion gauge and of vacuum itself, the chamber was first pumped with the ion gauge kept switched off all the time, and the samples characterized at the base pressure of  $1.3\times 10^{-6}$  mbar. The pressure was then stabilized at different levels up to  $3\times 10^{-4}$  mbar, by using a leak valve between the chamber and the ambient environment to gradually increase the pressure in the system. For each pressure level, the ion gauge was turned on for one to a few hundred seconds to see its effect on the sample. As shown in Fig. 2, we observe an increase of the sample resistance with time whenever the ion gauge is switched on (shaded regions), and an approximately constant resistance when the gauge is switched off. Interestingly, the speed at which the device resistance varies upon switching on the ion gauge increases with increasing pressure inside the chamber.

To understand the origin of the observed time dependence of the resistance, we measured the conductivity of our devices as a function of gate voltage, after having kept the devices in vacuum with the gauge turned on for different periods of time (Fig. 3). With increasing duration of the exposure to the ion gauge, we observe a systematic shift of the conductivity curve towards more negative gate voltages. Except for the slight broadening of the width of the conductivity dip at the charge neutrality point, the shape of the curve virtually does not change. The charge carrier mobility is thus not affected by the ion gauge effect. One may be superficially led to conclude that the shift originates from vacuum-induced

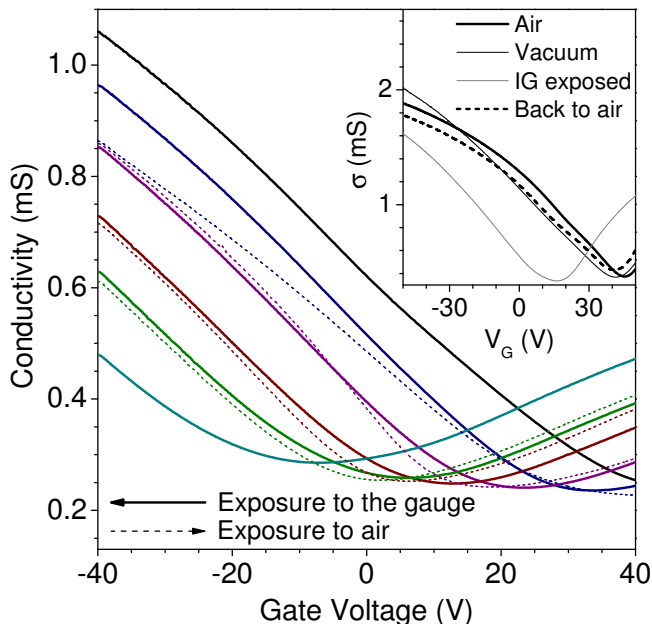


FIG. 3. Main panel: the thick solid lines – from right (black) to left (light blue) – show the conductivity  $\sigma$  versus gate voltage  $V_G$ , with each curve measured after having exposed the graphene device to the ion gauge (IG) for an increasingly long period of time. The shift of the charge neutrality point into negative  $V_G$  values indicates the occurrence of n-doping. The thin dashed lines (from left to right) illustrate the “recovery” of the sample upon exposure to air, showing the reversibility of the effect. Inset: similar measurements performed on an exfoliated graphene device show qualitatively similar trends (see main text).

desorption of adsorbates attached to the graphene sheet. However, this is clearly not the case because (i) a fast shift is only observed when the gauge is turned on (when the gauge is turned off a shift is still visible, but it is normally orders of magnitude slower and smaller); (ii) the charge neutrality point (i.e., the value of  $V_G$  for which the conductivity is minimum) shifts significantly into negative gate voltage values, an observation that is incompatible with only desorption of p-dopants; (iii) as we discuss in detail below, the effect is slower for better vacuum in the system. All these observations can only be explained if the vacuum gauge generates chemical species that propagate through the vacuum system and that act as n-dopants once they are absorbed onto the graphene sheet.

As shown by the dashed lines in Fig. 3, the effect is reversible after exposure to air, both in CVD graphene, previously annealed in vacuum to improve transport characteristics (causing p-dopant desorption, and thus a slight additional shift of the charge neutrality point), and in exfoliated, non-annealed graphene. In the latter, we measured the conductivity *vs* gate voltage characteristics in air, then in vacuum with the ion gauge off and with the ion gauge on, and finally after six days of recovery in air,

as shown in the inset of Fig. 3. We see that the vast majority of the doping effect occurs as a result of the exposure to the gauge, and that it is completely reversed after exposure to air.

To quantify the effect of the vacuum gauge we have estimated the doping rate  $dn/dt$ . The change in dopant concentration  $dn$  is obtained from the conductivity *vs* gate voltage curve ( $\sigma(V_G)$ ), using the known gate capacitance to convert the  $V_G$  shift of the charge neutrality point into a shift in carrier density. As shown in Fig. 4 for several CVD-grown samples (open symbols), we find that the doping rates  $dn/dt$  obtained in this way are roughly proportional to the pressure in the system, with a coefficient of proportionality  $\alpha$  of the order of  $10^{14} \text{ cm}^2\text{s}^{-1}\text{mbar}^{-1}$  (dashed line in Fig. 4). Devices made with standard exfoliated graphene (filled diamonds in Fig. 4) show qualitatively identical behavior, albeit with a slightly lower value of the coefficient  $\alpha$ . We thus conclude that the n-doping induced by the ion vacuum gauge is systematically present for all kinds of graphene devices (i.e., not only specific to our CVD grown samples).

The type of measurements just discussed can be used to provide a very direct, qualitative demonstration that the effect is indeed caused by the ion gauge. To this end, it is simply sufficient to compare the value of the parameter  $\alpha$  when repeating exactly the same experiment, but with the vacuum gauge mounted in different positions of the vacuum system as the only difference (the different positions are illustrated in the inset of Fig. 2). For a specific pressure in the vacuum system, the experimental values of  $\alpha$  thus obtained are the three data points in the shaded region of Fig. 4. The upper one (i.e. highest  $\alpha$ ) correspond to the case where the gauge is mounted directly on the probe station (position 1 in inset of Fig. 2).  $\alpha$  is an order of magnitude lower when the gauge is mounted in front of the chamber, on the pumping line (position 2 in inset of Fig. 2); it drops again over two orders of magnitude when the gauge is mounted close to the turbomolecular pump itself (position 3 in inset of Fig. 2). Thus, although the effect is seen irrespective of the position of the gauge in the system, its strength decreases when the gauge is mounted further away from the sample and closer to the inlet of the pump.

All our results are in line with observations reported earlier by Podzorov *et al.*<sup>19</sup> on a specific type of organic single-crystal transistors, in which the surface of the crystal where the transistor channel is formed is accessible to molecules present in the vacuum chamber. These authors also found a reversible and pressure-dependent n-doping generated from ion vacuum gauges, manifesting itself in a large shift of the device threshold voltage and – different from the case of graphene – in a strong carrier mobility suppression. Podzorov and coworkers attributed the effect to the creation of active species, possibly free radicals, on the hot gauge filament, which – when adsorbed on the organic crystal – simultaneously dope its surface (explaining the threshold voltage shift) and create local-

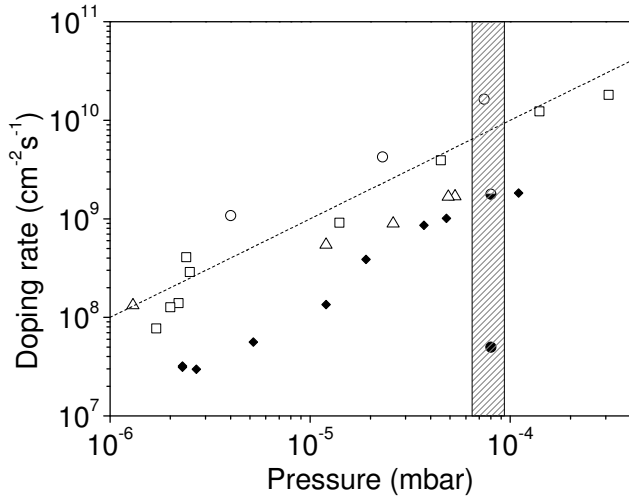


FIG. 4. Measured doping rate  $dn/dt$  versus pressure for different samples and ion gauge positions. Open symbols denote different CVD-grown graphene samples, and filled diamonds an exfoliated graphene device. All the samples show pressure dependent n-doping rates, with a coefficient of the order of  $10^{14} \text{ cm}^2 \text{ s}^{-1} \text{ mbar}^{-1}$  (dashed line). The three data points in the vertical shaded rectangle correspond to measurements of the same CVD-grown sample at the same pressure (approximately  $8 \times 10^{-5} \text{ mbar}$ ), but with the ion gauge mounted at different positions in the vacuum system, as indicated in the inset of Fig. 2. They show how the doping rate decreases from position (1) (open circle) to position (2) (half-filled circle) to position (3) (filled circle). The difference is due to the efficient evacuation of the active species created by the ion gauge when it is placed further away from the sample and closer to the pump.

ized electronic states in the gap of the organic semiconductor (accounting for the suppressed mobility). Indeed, such an explanation fully accounts for our observation on graphene as well (since graphene has no gap, the only visible effect is the shift of the charge neutrality point, and not a mobility suppression).

It is obviously important to be fully aware of the effect of ion vacuum gauges on graphene, since the majority of research groups working on this material performs experiment or measurements in vacuum systems where these ion vacuum gauges are very commonly employed, and kept turned on all the time. The gauge-induced n-doping can be very misleading when it comes to sample characterization. Graphene samples are usually p-doped if no annealing is done prior to the measurement, and the shift of the charge neutrality point toward smaller gate voltages could be interpreted as p-dopant desorption in vacuum, whereas it is actually the result of more dopants of the opposite sign produced by the ion gauge filament, being *adsorbed* onto the sample surface. Clearly, having p-dopants desorbed or compensated by n-dopants would lead to a very different situations if, for instance, local sample homogeneity is a relevant issue in the experiments. Furthermore, the vacuum gauge induced doping

effect occurs most intensely at high pressure, when the system is pumping prior to device measurement. Once base pressure is reached, the doping rate can become small enough to be unnoticeable over a short experimental time. It may therefore not be obvious that the ion gauge is the actual reason why n-doping is found in some samples. To avoid being misled, one should reduce to an absolute minimum the time of use of the ion gauge, and particularly avoid turning it on during the first pumping stages, when the pressure is still high (connecting the gauge far away from the sample and close to the pump might also be an option, although in this case recalibration is necessary to take into account the locally lower pressure directly along the pumping line).

The authors thank S. Muller and A. Ferreira for technical support, and J. Teyssier for his support on Raman spectroscopy. This work was funded by the Swiss National Science Foundation through the NCCR MaNEP and Division II grant 200020-138198.

- <sup>1</sup>A. K. Geim and K. S. Novoselov, Nat. Mater. **6**, 183 (2007).
- <sup>2</sup>A. H. Castro Neto, F. Guinea, N. M. R. Peres, K. S. Novoselov, and A. K. Geim, Rev. Mod. Phys. **81**, 109 (2009).
- <sup>3</sup>A. K. Geim, Science **324**, 1530 (2009).
- <sup>4</sup>W. Choi, I. Lahiri, R. Seelaboyina, and Y. S. Kang, Crit. Rev. Solid State **35**, 52 (2010).
- <sup>5</sup>K. S. Novoselov, V. I. Fal'ko, L. Colombo, P. R. Gellert, M. G. Schwab, and K. Kim, Nature **490**, 192 (2012).
- <sup>6</sup>X. Li, W. Cai, J. An, S. Kim, J. Nah, D. Yang, R. Piner, A. Velamakanni, I. Jung, E. Tutuc, S. K. Banerjee, L. Colombo, and R. S. Ruoff, Science **324**, 1312 (2009).
- <sup>7</sup>X. Li, C. W. Magnuson, A. Venugopal, J. An, J. W. Suk, B. Han, M. Borysiak, W. Cai, A. Velamakanni, Y. Zhu, L. Fu, E. M. Vogel, E. Voelkl, L. Colombo, and R. S. Ruoff, Nano Lett. **10**, 4328 (2010).
- <sup>8</sup>M. P. Levendoff, C. S. Ruiz-Vargas, S. Garg, and J. Park, Nano Lett. **9**, 4479 (2009).
- <sup>9</sup>S. Bae, H. Kim, Y. Lee, X. Xu, J.-S. Park, Y. Zheng, J. Balakrishnan, T. Lei, H. Ri Kim, Y. I. Song, Y.-J. Kim, K. S. Kim, B. Ozyilmaz, J.-H. Ahn, B. H. Hong, and S. Iijima, Nat. Nanotechnol. **5**, 574 (2010).
- <sup>10</sup>A. Reina, X. Jia, J. Ho, D. Nezich, H. Son, V. Bulovic, M. S. Dresselhaus, and J. Kong, Nano Lett. **9**, 30 (2009).
- <sup>11</sup>A. Reina, S. Thiele, X. Jia, S. Bhaviripudi, M. Dresselhaus, J. Schaefer, and J. Kong, Nano Res. **2**, 509 (2009).
- <sup>12</sup>K. S. Kim, Y. Zhao, H. Jang, S. Y. Lee, J. M. Kim, K. S. Kim, J. . Ahn, P. Kim, J. . Choi, and B. H. Hong, Nature **457**, 706 (2009).
- <sup>13</sup>K. S. Novoselov, A. K. Geim, S. V. Morozov, D. Jiang, Y. Zhang, S. V. Dubonos, I. V. Grigorieva, and A. A. Firsov, Science **306**, 666 (2004).
- <sup>14</sup>Small particles can be formed during graphene growth, as previously reported in Ref. 15. Using scanning electron microscopy, we have additionally observed that growth conditions can modify the nanoparticle density, size (from 100 nm to 1  $\mu\text{m}$ ), and shape (from rounded to tetragonal). We suggest that, because of their tetragonal shape, the observed nanoparticles are nanodiamonds, although the presence of Cu residues cannot be completely excluded.
- <sup>15</sup>X. Liang, B. A. Sperling, I. Calizo, G. Cheng, C. A. Hacker, Q. Zhang, Y. Obeng, K. Yan, H. Peng, Q. Li, X. Zhu, H. Yuan, A. R. Hight Walker, Z. Liu, L.-m. Peng, and C. A. Richter, ACS Nano **5**, 9144 (2011), Here we used HCl 30 % with a few drops of  $\text{H}_2\text{O}_2$  30 % as the Cu etchant.
- <sup>16</sup>A. C. Ferrari, J. C. Meyer, V. Scardaci, C. Casiraghi, M. Lazzeri, F. Mauri, S. Piscanec, D. Jiang, K. S. Novoselov, S. Roth, and A. K. Geim, Phys. Rev. Lett. **97**, 187401 (2006).

- <sup>17</sup>A. Reina, X. Jia, J. Ho, D. Nezich, H. Son, V. Bulovic, M. S. Dresselhaus, and J. Kong, *Nano Lett.* **9**, 30 (2009).
- <sup>18</sup>A. C. Ferrari, *Solid State Commun.* **143**, 47 (2007).
- <sup>19</sup>V. Podzorov, E. Menard, S. Pereversev, B. Yakshinsky, T. Madey, J. A. Rogers, and M. E. Gershenson, *Appl. Phys. Lett.* **87**, 093505 (2005).